Biochimica et Biophysica Acta 1808 (2011) 1219–1229

Contents lists available at ScienceDirect

Biochimica et Biophysica Acta

journal homepage: www.elsevier.com/locate/bbamem

Membrane interaction of segment H1 ($NS4B_{H1}$) from hepatitis C virus non-structural protein 4B

M. Francisca Palomares-Jerez, José Villalaín *

Instituto de Biología Molecular y Celular, Universidad Miguel Hernández, E-03202 Elche-Alicante, Spain

ARTICLE INFO

Article history:
Received 9 November 2010
Received in revised form 15 December 2010
Accepted 23 December 2010
Available online 31 December 2010

Keywords:
HCV replication
HCV
Lipid–peptide interaction
Membranous web
NS4B H1

ABSTRACT

NS4B protein from hepatitis C virus (HCV) is a highly hydrophobic protein inducing a rearrangement of endoplasmic reticulum membranes responsible of the HCV replication process. Different helical elements have been found in the N- and C- terminal domains of the protein, which seem to be responsible for many key aspects of the viral replication process. In this work we have carried out a study of the binding and interaction with model biomembranes of peptide $NS4B_{H1}$, patterned after segment H1, one of these C-terminal previously identified segments. We show that $NS4B_{H1}$ partitions into phospholipid membranes; its membrane activity is modulated by lipid composition, interacting preferentially with negatively charged phospholipids as well as with sphingomyelin. Furthermore, the change in its sequence prevents the resulting peptide from interacting with the membrane. These data would support its role in the interaction of NS4B with the membrane and suggest that the region where this peptide resides could be involved in the membrane alteration which must occur in the HCV replication and/or assembly process.

1. Introduction

The emergence and resurgence of many animal and human viral pathogens have many causes, but one of the most important is the lack of effective antiviral therapies [1]. This is the case of hepatitis C virus (HCV), an enveloped positive single-stranded RNA virus, which belongs to the genus *Hepacivirus* within the family *Flaviviridae*, the major cause of liver disease. With more than 180 million people infected worldwide [2], its high persistence, no protective vaccine and limited therapeutic agents, this disease has emerged as a serious healthcare problem on a global scale [3,4].

HCV entry into the host cell is achieved by the fusion of viral and cellular membranes, replicates its genome in a membrane-associated replication complex, and morphogenesis has been suggested to take place in the endoplasmic reticulum (ER) or modified ER membranes [5]. The variability of the HCV proteins gives the virus the ability to escape the host immune surveillance system and notably hampers the development of an efficient vaccine. HCV has a single-stranded genome which encodes a polyprotein, cleaved by a combination of cellular and viral proteases to produce the mature structural and non-structural (NS) proteins [3,6]. Details about HCV replication process remain largely unclear, but most if not all of the HCV non-structural proteins (NS) proteins are involved and function in a complex web of protein-protein interactions [6,7]. The fact that all NS proteins are localized together with newly synthesized viral RNA on the ER or membranes originating from it [8–10] supports this hypothesis.

Non-structural protein 4B (NS4B) protein, a fundamental player in the HCV replicative process and the least characterized HCV protein, is a highly hydrophobic protein associated with membranes of an ER-derived modified compartment [11]. It has recently been shown that NS4B is palmitoylated in the C-terminal region of the protein; its N-terminal cytoplasmic region has potent polymerization activity [12] and is engaged in virus assembly and release [13]. Interestingly, the expression of NS4B induces the formation of the so called membranous web [14], which has been postulated to be the HCV RNA replication complex. Thus, a function of NS4B might be to induce a specific membrane alteration that serves as a scaffold for the formation of the HCV replication complex and therefore has a critical role in the HCV

Abbreviations: 16-NS, 16-Doxyl-stearic acid; 5-NS, 5-Doxyl-stearic acid; BPI, Bovine brain L-α-phosphatidylinositol; BPS, Bovine brain L-α-phosphatidylserine; CF, 5-Carboxyfluorescein; CHOL, Cholesterol; CL, Bovine heart cardiolipin; DMPA, 1,2-Dimyristoyl-*sn*-glycero-3-phosphatidic acid; DMPC, 1,2-Dimyristoyl-*sn*-glycero-3-phosphatidylcholine; DMPG, 1,2-Dimyristoyl-*sn*-glycero-3-[phospho-rac-glycerol]; DMPS, 1,2-Dimyristoyl-*sn*-glycero-3-phosphatidylserine; DPH, 1,6-Diphenyl-1,3,5-hexatriene; DSC, Differential scanning calorimetry; EPA, Egg L-α-phosphatidic acid; EPC, Egg L-α-phosphatidylcholine; EPG, Egg L-α-phosphatidylglycerol; ER, Endoplasmic reticulum; ESM, Egg sphingomyelin; HCV, Hepatitis C virus; IR, Infrared spectroscopy; LUV, Large unilamellar vesicles; MLV, Multilamellar vesicles; NS, Non-structural protein; PSM, N-palmitoyl-D-erythro-sphingosylphosphorylcholine; SUV, Small unilamellar vesicles; TFE, Trifluoroethanol; T_m, Temperature of the gel-to-liquid crystalline phase transition; TMA-DPH, 1-(4-Trimethylammoniumphenyl)-6-phenyl-1,3,5-hexatriene; TPE, Egg trans-esterified L-α-phosphatidylethanolamine

* Corresponding author. Tel.: +34 966 658 762; Fax +34 966 658 758.
E-mail address: jvillalain@umh.es (J. Villalaín).

0005-2736/$ – see front matter © 2010 Elsevier B.V. All rights reserved.
doi:10.1016/j.bbamem.2010.12.023

cycle. Due to the high hydrophobic nature of NS4B, a detailed structure determination of this protein is very difficult. NS4B is likely to be anchored to the membrane and be an integral membrane protein with four or more transmembrane domains [11,15,16].

The C-terminal part of NS4B reveals significant similarities throughout all investigated viruses of the *Flaviviridae* family. Two α-helical elements have been predicted, the first α-helix (H1) approximately from amino acid 1912 to 1924 and the second α-helix (H2) approximately from amino acid 1940 to 1963, pointing out to a yet unknown common function of the C-terminal globular part in *Flaviviridae* [17]. These α-helical elements have been reported to be potential targets of HCV replication inhibitors [18]. Previous studies from our group studying the effect of NS4B-derived peptide libraries on model membrane integrity have helped us to understand the mechanisms underlying the interaction between NS4B and membranes [19]. These results allowed us to propose the location of different segments in these proteins that are implicated in protein-lipid and protein-protein interactions. One of those segments was located where the H1 region resides. In the present study, we report the binding and interaction of a peptide corresponding to the first of the two predicted amphipathic helices (peptide $NS4B_{H1}$) both in aqueous solution and in the presence of different membrane model systems and define it as a membrane interacting domain. We show that $NS4B_{H1}$ strongly partitions into phospholipid membranes, interacts with them, and is located at the membrane interface, modulates the phospholipid phase behavior and changes its secondary structure upon binding to the membrane. These results would suggest that this NS4B element is an essential constituent of the interaction between the protein and the membrane and might shed light into the specific function of the NS4B protein in the viral cycle.

2. Materials and methods

2.1. Reagents

Strictly speaking, HCV NS4B spans from residue 1712 to residue 1972 of the HCV polyprotein precursor. However, and to avoid any confusion, in this work we are going to use the HCV NS4B numbering scheme, i.e., from residue 1 to residue 261. Peptides $NS4B_{H1}$ (sequence ^{198}GEGAVQWMNRLIAFASRG^{215}) and scrambled peptide $NS4B_{H1SC}$ (SAVRNAFIGQGMGRWEAL) were synthesized with N-terminal acetylation and C-terminal amidation on an automatic multiple synthesizer (Genemed Synthesis, San Antonio, TX, USA). The peptide was purified by reverse-phase high-performance liquid chromatography (Vydac C-8 column, 250×4.6 mm, flow rate 1 ml/min, solvent A, 0.1% trifluoroacetic acid, solvent B, 99.9 acetonitrile and 0.1% trifluoroacetic acid) to >95% purity, and its composition and molecular mass were confirmed by amino acid analysis and mass spectrometry. Since trifluoroacetate has a strong infrared absorbance at approximately 1673 cm^{-1}, which interferes with the characterization of the peptide Amide I band [20], residual trifluoroacetic acid, used both in peptide synthesis and in the high-performance liquid chromatography mobile phase, was removed by four lyophilisation/solubilisation cycles in 10 mM HCl [21]. Peptide was solubilized in water/TFE at 50% (v/v). Bovine brain phosphatidylserine (BPS), bovine liver L-α-phosphatidylinositol (BPI), cholesterol (CHOL), egg phosphatidic acid (EPA), egg L-α-phosphatidylcholine (EPC), egg sphingomyelin (ESM), egg trans-sterified L-α-phosphatidylethanolamine (TPE), tetramyristoyl cardiolipin (CL), 1,2-dimyristoylphosphatidylserine (DMPS), 1,2-dimyristoylphosphatidic acid (DMPA), 1,2-dimyristoylphosphatidylcholine (DMPC), 1,2-dimyristoylphosphatidylglycerol (DMPG) and N-palmitoyl-D-erythro-sphingosylphosphorylcholine (PSM) were obtained from Avanti Polar Lipids (Alabaster, AL, USA). The lipid composition of the synthetic ER was EPC/CL/BPI/TPE/BPS/EPA/ESM/Chol at a molar ratio of 59:0.37:7.4:18:3.1:1.2:3.4:7.8 [22]. 5-Carboxyfluorescein (CF, >95% by HPLC), 5-doxyl-stearic acid (5-NS), 16-doxyl-stearic acid (16-NS), deuterium oxide (99.9%), Triton X-100, EDTA and HEPES were purchased from Sigma-Aldrich (Madrid, Spain). 1,6-Diphenyl-1,3,5-hexatriene (DPH), and 1-(4-trimethylammoniumphenyl)-6-phenyl-1,3,5-hexatriene (TMA-DPH) were obtained from Molecular Probes (Eugene, OR). All other chemicals were commercial samples of the highest purity available (Sigma-Aldrich, Madrid, Spain). Water was deionized, twice-distilled and passed through a Milli-Q equipment (Millipore Ibérica, Madrid, Spain) to a resistivity higher than 18 MΩ cm.

2.2. Vesicle preparation

Aliquots containing the appropriate amount of lipid in chloroform-methanol (2:1 vol/vol) were placed in a test tube, the solvents were removed by evaporation under a stream of O_2-free nitrogen, and finally, traces of solvents were eliminated under vacuum in the dark for >3 h. The lipid films were resuspended in an appropriate buffer and incubated either at 25 °C or 10 °C above the phase transition temperature (T_m) with intermittent vortexing for 30 min to hydrate the samples and obtain multilamellar vesicles (MLV). The samples were frozen and thawed five times to ensure complete homogenization and maximization of peptide/lipid contacts with occasional vortexing. Large unilamellar vesicles (LUV) with a mean diameter of 0.1 μm were prepared from MLV by the extrusion method [23] using polycarbonate filters with a pore size of 0.1 μm (Nuclepore Corp., Cambridge, CA, USA). For infrared spectroscopy, aliquots containing the appropriate amount of lipid in chloroform/methanol (2:1, v/v) were placed in a test tube containing 200 μg of dried lyophilized peptide. After vortexing, the solvents were removed by evaporation under a stream of O_2-free nitrogen, and finally, traces of solvents were eliminated under vacuum in the dark for more than 3 h. The samples were hydrated in 100 μl of D_2O buffer containing 20 mM HEPES, 100 mM NaCl, 0.1 mM EDTA, pH 7.4 and incubated at 10 °C above the T_m of the phospholipid mixture with intermittent vortexing for 45 min to hydrate the samples and obtain MLV. The samples were frozen and thawed as above. Finally the suspensions were centrifuged at 15,000 rpm at 25 °C for 10 min to remove the possibly peptide unbound to the membranes. The pellet was resuspended in 25 μl of D_2O buffer and incubated for 45 min at 10 °C above the T_m of the lipid mixture, unless stated otherwise. The phospholipid and peptide concentrations were measured by methods described previously [24,25].

2.3. Membrane leakage and peptide binding to vesicles

LUVs with a mean diameter of 0.1 μm were prepared as indicated above in buffer containing 10 mM Tris, 20 mM NaCl, pH 7.4, and CF at a concentration of 40 mM. Non-encapsulated CF was separated from the vesicle suspension through a Sephadex G-50 filtration column (Pharmacia, Uppsala, Sweden) eluted with buffer containing 10 mM Tris, 100 mM NaCl, 1 mM EDTA, pH 7.4. Membrane rupture (leakage of intraliposomal CF) was assayed by treating the probe-loaded liposomes (final lipid concentration, 0.125 mM) with the appropriate amounts of peptide on microtiter plates using a microplate reader (FLUORstar; BMG Labtech, Offenburg, Germany), stabilized at 25 °C with the appropriate amounts of peptide, each well containing a final volume of 170 μl. The medium in the microtiter plates was continuously stirred to allow the rapid mixing of peptide and vesicles. One hundred percent release was achieved by adding Triton X-100 to either the microtiter plate to final concentration of 0.5% (w/w). Changes in fluorescence intensity were recorded with excitation and emission wavelengths set at 492 and 517 nm, respectively. Leakage was quantified on a percentage basis as previously described [26,27]. Steady-state fluorescence spectra were recorded in a SLM Aminco 8000 C spectrofluorometer with excitation and emission wavelengths of 290 and 348 nm, respectively, and 4 nm spectral bandwidths. Measurements were carried out in 10 mM Tris, 100 mM NaCl, EDTA 0.1 mM, pH 7.4. Intensity values were corrected for dilution, and the

scatter contribution was derived from lipid titration of a vesicle blank. Partition coefficients K_P (i.e. the amount of peptide bound to the bilayer as a fraction of the total peptide present in the system) were obtained as described previously [28–30].

2.4. Acrylamide quenching of Trp emission, quenching with lipophylic depth probes and steady-state fluorescence anisotropy

Aliquots from a 4 M solution of the water-soluble quencher were added to the solution-containing peptide in the presence and absence of liposomes at a peptide/lipid molar ratio of 1:100. The results obtained were corrected for dilution and the scatter contribution was derived from acrylamide titration of a vesicle blank. Aliquots of TMA-DPH or DPH in *N,N′*-dimethylformamide were directly added into MLVs formed in 10 mM Tris, 100 mM NaCl, EDTA 0.1 mM, pH 7.4 to obtain a probe/lipid molar ratio of 1:500. Samples were incubated for 15 or 60 min when TMA-DPH or DPH were used, respectively, 10 °C above the gel to liquid-crystalline phase transition temperature T_m of the phospholipid mixture. Afterwards, the peptides were added to obtain a peptide/lipid molar ratio of 1:15 and incubated 10 °C above the T_m of each lipid for 1 h, with occasional vortexing. All fluorescence studies were carried using 5 mm × 5 mm quartz cuvettes in a final volume of 400 μl (315 μM lipid concentration). The steady-state fluorescence anisotropy was measured with an automated polarization accessory using a Varian Cary Eclipse fluorescence spectrometer, coupled to a Peltier for automatic temperature change. Samples were excited at 360 nm (slit width, 5 nm) and fluorescence emission was recorded at 430 nm (slit width, 5 nm). Quenching studies with lipophylic probes were performed by successive addition of small amounts of 5-NS or 16-NS in ethanol to peptide samples incubated with LUV. The final concentration of ethanol was kept below 2.5% (v/v) to avoid any significant bilayer alterations. After each addition an incubation period of 15 min was kept before the measurement. The data were analyzed as previously described [27]. The Stern–Volmer quenching constant, K_{SV}, obtained from the Stern–Volmer equation, represents the quencher concentration at which 50% of the intensity is quenched and it is therefore a measure of the accessibility of Trp to the quencher molecule [31].

2.5. Differential scanning calorimetry

MLVs were formed as stated above in 20 mM HEPES, 100 mM NaCl, 0.1 mM EDTA, pH 7.4. The peptide was added to obtain a peptide/lipid molar ratio of 1:15. The final volume was 1.2 ml (0.5 mM lipid concentration), and incubated 10 °C above the T_m of each phospholipid for 1 h with occasional vortexing. DSC experiments were performed in a VP-DSC differential scanning calorimeter (MicroCal LLC, MA) under a constant external pressure of 30 psi in order to avoid bubble formation, and samples were heated at a constant scan rate of 60 °C/h. Experimental data were corrected from small mismatches between the two cells by subtracting a buffer baseline prior to data analysis. The excess heat capacity functions were the analyzed by using Origin 7.0 (Microcal Software). The thermograms were defined by the onset and completion temperatures of the transition peaks obtained from heating scans. In order to avoid artifacts due to the thermal history of the sample, the first scan was never considered; second and further scans were carried out until a reproducible and reversible pattern was obtained.

2.6. Infrared spectroscopy

Approximately 25 μl of a pelleted sample in D_2O was placed between two CaF_2 windows separated by 56-μm-thick Teflon spacers in a liquid demountable cell (Harrick, Ossining, NY). The spectra were obtained in a Bruker IFS55 spectrometer using a deuterated triglycine sulfate detector. Each spectrum was obtained by collecting 250 interferograms with a nominal resolution of 2 cm^{-1}, transformed using triangular apodization and, in order to average background spectra between sample spectra over the same time period, a sample shuttle accessory was used to obtain sample and background spectra. The spectrometer was continuously purged with dry air at a dew point of -40 °C in order to remove atmospheric water vapour from the bands of interest. All samples were equilibrated at the lowest temperature for 20 min before acquisition. An external bath circulator, connected to the infrared spectrometer, controlled the sample temperature. For temperature studies, samples were scanned using 2 °C intervals and a 2-min delay between each consecutive scan. The data were analyzed as previously described [26,30].

3. Results

Through the analysis of hydrophobicity, hydrophobic moments and interfacial hydrophobicity distribution along the NS4B sequence as well as the effect of a HCV NS4B derived peptide library on membrane rupture, we have previously identified two zones of highly hydrophobic character [19]. These zones approximately correspond to the proposed α-helical elements predicted in the C-terminal part of NS4B, i.e., H1, of approximately 13 residues in length, and H2, comprising approximately 23 residues [17]. Since they could mediate the interaction with similar domains of other HCV NS proteins, with other host proteins or with the membrane it is very interesting to investigate the binding and interaction with membrane model systems of these highly hydrophobic regions of NS4B [3]. As shown in Table 1, the region where H1 resides is significantly conserved among the major genotypes of HCV. The conservation of this pattern across different strains of HCV indicates that this sequence is likely to be an important region in NS4B protein. Taking into account these results, as well as the above mentioned literature data concerning the membrane-mediated HCV replication process modulated by NS4B, we have performed an in-depth study of H1 peptide (from residue 198 to residue 215, HCV NS4B numbering), i.e., peptide $NS4B_{H1}$ (Table 1). In order to discern any differences between the $NS4B_{H1}$ sequence and its amino acid composition, we have studied also a scrambled peptide, $NS4B_{H1SC}$ (Table 1). We have investigated their binding and interaction with different membrane model systems, as well as characterized the structural changes taking place in both the peptides and the phospholipid molecules.

3.1. Membrane leakage

In order to explore the possible interaction of the $NS4B_{H1}$ peptide with phospholipid model membranes, we studied the effect of the $NS4B_{H1}$ and $NS4B_{H1SC}$ peptides on the release of encapsulated fluorophores trapped inside model membranes composed of diverse lipids [32,33]. The extent of leakage observed at different lipid-to-peptide ratios and the effect of lipid composition is shown in Fig. 1A. The $NS4B_{H1}$ peptide was able to induce the release of the internal contents of the liposomes in a dose-dependent manner. The $NS4B_{H1}$ peptide induced a high percentage of leakage (90%), even at lipid/peptide ratios of 30:1, for liposomes composed of EPC/EPA at a molar ratio of 5:2. Lower but significant leakage values were observed for liposomes containing EPC (65%), EPA/CHOL at a molar ratio of 5:1 (60%), BPS/CHOL at a molar ratio of 5:1 (50%), EPC/BPS/CHOL at a molar ratio of 5:3:1 (50%), and BPS/CHOL at a molar ratio of 5:1 (45%). Lower values were obtained for liposomes composed of synthetic ER membranes (35%), EPC/TPE/CHOL at a molar ratio of 5:3:1 (35%), EPC/CHOL at a molar ratio of 5:1 (20%) and EPC/ESM/CHOL at a molar ratio of 5:1:1 (20%). These results indicate that the peptide affects more significantly membranes containing negatively charged phospholipids rather than those containing zwitterionic ones. Remarkably, the scrambled peptide $NS4B_{H1SC}$ did not produce any significant leakage for any of the liposome compositions as shown in Fig. 1A. These data

Table 1
Alignment (clustalw2) for reference strains representing the major genotypes of hepatitis C virus. Alignment of residues 198–215 (HCV NS4B numbering) is shown. The consensus sequence is shown beneath the alignment. Symbol * stand for identical residues. The sequence of the peptides studied in this work is emphasized in bold.

GENOTYPE_STRAIN	SEQUENCE
2c_BEBE1	GEGAVQWMNRLIAFASRG
2k_VAT96	GEGAVQWMNRLIAFASRG
2b_JPUT971017	GEGAVQWMNRLIAFASRG
2i_D54	GEGAVQWMNRLIAFASRG
2a_HC-J6	GEGAVQWMNRLIAFASRG
1a_1	GEGAVQWMNRLIAFASRG
1a_H77	GEGAVQWMNRLIAFASRG
1c_HC-G9	GEGAVQWMNRLIAFASRG
1b_Con1	GEGAVQWMNRLIAFASRG
1b_HC-J4	GEGAVQWMNRLIAFASRG
1g_1804	GEGAVQWMNRLIAFASRG
4a_ED43	GEGAVQWMNRLIAFASRG
4d_24	GEGAVQWMNRLIAFASRG
4k_PB65185	GEGAVQWMNRLIAFASRG
4f_CM_DAV9905	GEGAVQWMNRLIAFASRG
3a_NZL1	GEGAVQWMNRLIAFASRG
3b_Tr-Kj	GEGAVQWMNRLIAFASRG
3k_JK049	GEGAVQWMNRLIAFASRG
5a_EUH1480	GEGAVQWMNRLIAFASRG
6c_Th846	TEGAAQWMNRLIAFASRG
6d_VN235	SEGATQWMNRLIAFASRG
6t_D49	TEGAAQWMNRLIAFASRG
6e_D42	SEGAAQWMNRLIAFASRG
6f_C-0044	SEGANQWMNRLIAFASRG
6a_D85	SEGATQWMNRLIAFASRG
6h_VN004	SEGATQWMNRLIAFASRG
6k_VN405	AEGATQWMNRLIAFASRG
6g_JK046	SEGAAQWMNRLIAFASRG
6a_6a33	AEGANQWMNRLIAFASRG
6b_Th580	SEGANQWMNRLIAFASRG
7a_QC69	SEGVTQWMNRLIAFASRG
consensus	**.**********
$NS4B_{H1}$	**GEGAVQWMNRLIAFASRG**
$NS4B_{H1SC}$	**SAVRNAFIGQGMGRWEAL**

show that the $NS4B_{H1}$ sequence but not the amino acid composition is crucial to observe any membranotropic effect.

Interestingly, it has been shown that the active replication complexes of HCV might be localized in lipid rafts, composed predominantly of ESM and CHOL [34,35]. Fig. 1B shows the extent of leakage for liposomes composed of different molar ratios of EPC, ESM and CHOL. Significant leakage values were observed for EPC/ESM/CHOL membranes at molar ratios of 5:2:0, 5:5:1, 5:4:1 and 5:3:1 (70–90%). Lower but significant values were observed for EPC/ESM/CHOL membranes at molar ratios of 5:2:1 and 5:2:2 (40–60%). For EPC/ESM/CHOL membranes at molar ratios of 5:1:1, 5:2:3 and 5:2:4 leakage values were observed between 5 and 20%. As a general trend, the higher the ESM content and the lower the CHOL, the higher the leakage is (Fig. 1C). For different lipid/peptide ratios this trend is clearly visible, since increasing the relative content of ESM and at the same time decreasing the relative content of CHOL, the leakage values increases steadily (Fig. 1C).

Since the NS4B protein is associated with membranes of the ER or an ER-derived modified compartment [11], we have studied the effect of the $NS4B_{H1}$ peptide on membrane rupture using a complex lipid composition resembling the ER membrane as well as the effect of each component of the complex mixture (Fig. 1D). Since the synthetic ER complex membrane used in the previous experiments was composed of EPC, CL, BPI, TPE, BPS, EPA, ESM and CHOL at a molar ratio of 59:0.37:7.4:18:3.1:1.2:3.4:7.8 [22], we have designed an ER synthetic membrane composed of EPC/CL/BPI/TPE/BPS/EPA/ESM/CHOL at a molar ratio of 58:6:6:6.6:6:6:6 ($ER^{58:6}$). This complex mixture is very useful in order to study the effect of each lipid component on the interaction of the peptide with the membrane. As shown in Fig. 1D, the $NS4B_{H1}$ peptide was able of rupturing the synthetic ER membranes significantly, since, at lipid/peptide ratios of 25:1 and 30:1, 95–85% of leakage was attained. Removing either TPE or CL from the mixture hardly any effect was observed on leakage, since the leakage values observed were about 85%. When CHOL, EPA and BPI were removed from the mixture, leakage values between 40 and 70% were found. A more significant effect was observed when ESM and BPS were eliminated from the mixture, since leakage values of about 20–30% were observed for lipid/peptide ratios of 25:1 and 30:1 (Fig. 1D). These results confirm the specific effect of the $NS4B_{H1}$ peptide on negatively charged phospholipids as well as sphingomyelin containing membranes, since their removal decreased significantly the observed effect in the synthetic ER complex membrane.

3.2. Binding of $NS4B_{H1}$ peptide to lipid vesicles

The ability of the $NS4B_{H1}$ peptide to interact with membranes was determined from fluorescence studies of the peptide intrinsic Trp [36] using liposomes containing different phospholipid compositions at different lipid/peptide ratios (Fig. 2A). In order to observe any specific interaction of the peptide with any specific type of lipid, the model membranes were composed of zwitterionic and negatively charged phospholipids as well as ESM and CHOL at different molar ratios. The Trp fluorescence intensity of the $NS4B_{H1}$ peptide greatly increased upon increasing the lipid/peptide ratio using membranes composed of either EPA/CHOL or BPS/CHOL at molar ratios of 5:1, indicating a significant change on the environment of the Trp moiety of the peptide in the presence of these negatively charged lipids (Fig. 2A). A significant change on the Trp fluorescence intensity of the $NS4B_{H1}$ peptide was observed also for membranes composed of EPC/EPA at a molar ratio of 5:2; smaller but significant changes were observed for EPC/BPS at a molar ratio of 5:2 and EPC/ESM/CHOL at a molar ratio of 5:3:1 (Fig. 2A). The change on the Trp fluorescence of the peptide has permitted us to obtain its partition coefficient, K_P, for different membrane compositions (Table 2). K_P values in the range 10^5 were obtained, indicating that the peptide was bound to the membrane surface with high affinity [28,36–38]. If we suppose that the fluorescence intensity of the Trp residue is related to the peptide location in the membrane [31], the peptide insert more deeply in membranes composed of negatively charged phospholipids than on membranes composed of zwitterionic ones. The $NS4B_{H1}$ peptide has a positive net formal charge of +1 at neutral pH, so that an electrostatic effect might be the reason to observe a significant increase of Trp fluorescence in the presence of anionic membranes than in the presence of membranes containing zwitterionic phospholipids. However, electrostatic attraction is not the only element that is playing a role, since the $NS4B_{H1SC}$ peptide, having the same amino acid composition, i.e., the same positive net formal charge of +1 at neutral pH, is affected much less significantly in the presence of membranes containing negatively charged phospholipids than the $NS4B_{H1}$ peptide (not shown). Comparing the data shown in Figs. 1A and 2A, a relatively good relationship exists between the Trp fluorescence intensity of the peptides and membrane rupture, i.e., the deeper location of the peptides, the higher the CF leakage is.

3.3. Location and penetration of $NS4B_{H1}$ peptide in the bilayer

To assess the accessibility of the Trp residue of the $NS4B_{H1}$ peptide to the aqueous environment before and after binding to membranes having different phospholipid compositions, the water-soluble quencher acrylamide, an efficient neutral quencher probe [29] was used. Stern–Volmer plots for the quenching of Trp by acrylamide, recorded in the absence and presence of lipid vesicles, are shown in Fig. 2B and the resultant Stern–Volmer constants are presented in Table 2. Linear Stern–Volmer plots indicate that the Trp residue is fairly accessible to acrylamide, and in all cases, the quenching of the peptide Trp residue showed an acrylamide dependent concentration

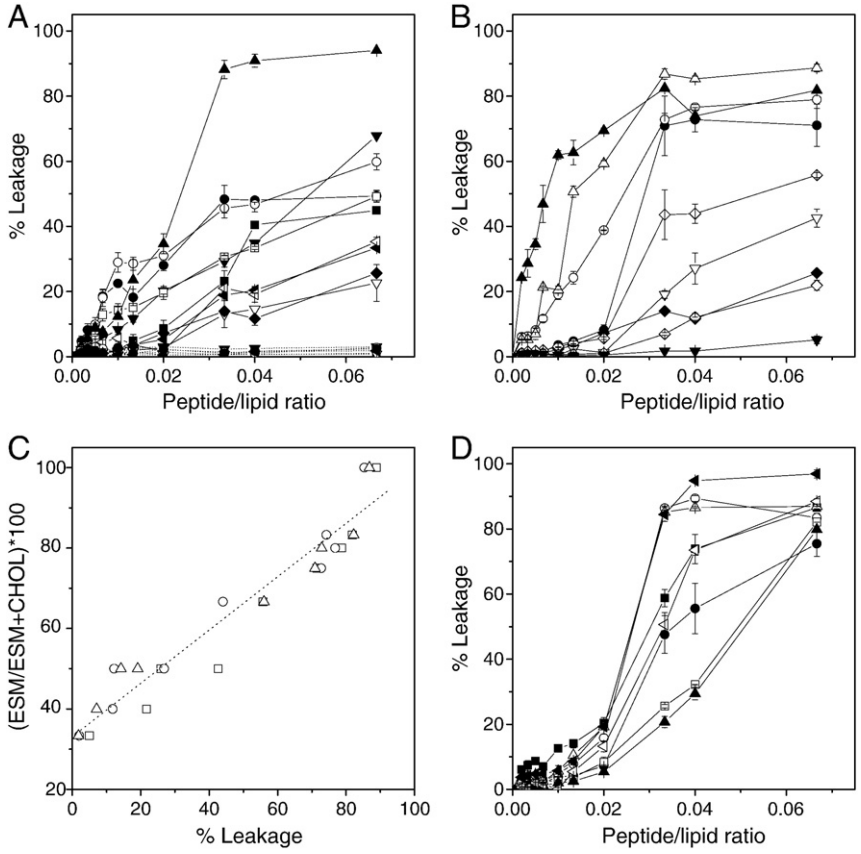

Fig. 1. (A) Effect of the $NS4B_{H1}$ (continuous line) and $NS4B_{H1SC}$ (dotted line) peptides on the release (membrane rupture) of CF for different lipid compositions. The lipid compositions used were ER (◀), EPC (▼), BPS/CHOL at a molar ratio of 5:1 (■), EPA/CHOL at a molar ratio of 5:1 (○), EPC/CHOL at a molar ratio of 5:1 (▽), EPC/ESM/CHOL at a molar ratio of 5:1:1 (♦), EPC/EPA at a molar ratio of 5:2 (▲), EPC/BPS at a molar ratio of 5:2 (□), EPC/BPS/CHOL at a molar ratio of 5:3:1 (●) and EPC/TPE/CHOL at a molar ratio of 5:3:1 (◁). The ER complex lipid mixture is composed of EPC/CL/BPI/TPE/BPS/EPA/ESM/CHOL at a molar ratio of 59:0.37:7.4:18:3.1:1.2:3.4:7.8 [22]. (B) Effect of the $NS4B_{H1}$ peptide on the release (membrane rupture) of CF for lipid compositions containing different molar ratios of EPC, ESM and CHOL. The lipid compositions used were EPC/ESM/CHOL at a molar ratio of 5:1:1 (♦), EPC/ESM/CHOL at a molar ratio of 5:3:1 (●), EPC/ESM/CHOL at a molar ratio of 5:2:1 (◊), EPC/ESM/CHOL at a molar ratio of 5:4:1 (○), EPC/ESM/CHOL at a molar ratio of 5:5:1 (▲), EPC/ESM/CHOL at a molar ratio of 5:2:0 (△), EPC/ESM/CHOL at a molar ratio of 5:2:2 (▽), EPC/ESM/CHOL at a molar ratio of 5:2:3 (◊), and EPC/ESM/CHOL at a molar ratio of 5:2:4 (▼). (C) Relationship between the relative content of ESM and CHOL versus membrane rupture for lipid/peptide molar ratios of 30:1 (△), 25:1 (○) and 15:1 (□). The dotted line is the fit to the ESM data ($R^2 = 0.9278$). (D) Effect of the $NS4B_{H1}$ peptide on the release (membrane rupture) of CF for the $ER^{58:6}$ complex lipid mixture (EPC/CL/BPI/TPE/BPS/EPA/ESM/CHOL at a molar ratio of 58:6:6:6:6.6:6:6:6) and its variations. The lipid compositions used were $ER^{58:6}$ (◀), $ER^{58:6}$ minus BPI (●), $ER^{58:6}$ minus TPE (○), $ER^{58:6}$ minus CHOL (■), $ER^{58:6}$ minus ESM (□), $ER^{58:6}$ minus BPS (▲), $ER^{58:6}$ minus CL (△) and $ER^{58:6}$ minus EPA (◁). Vertical bars indicate standard deviations of the mean of triplicate samples. See text for details.

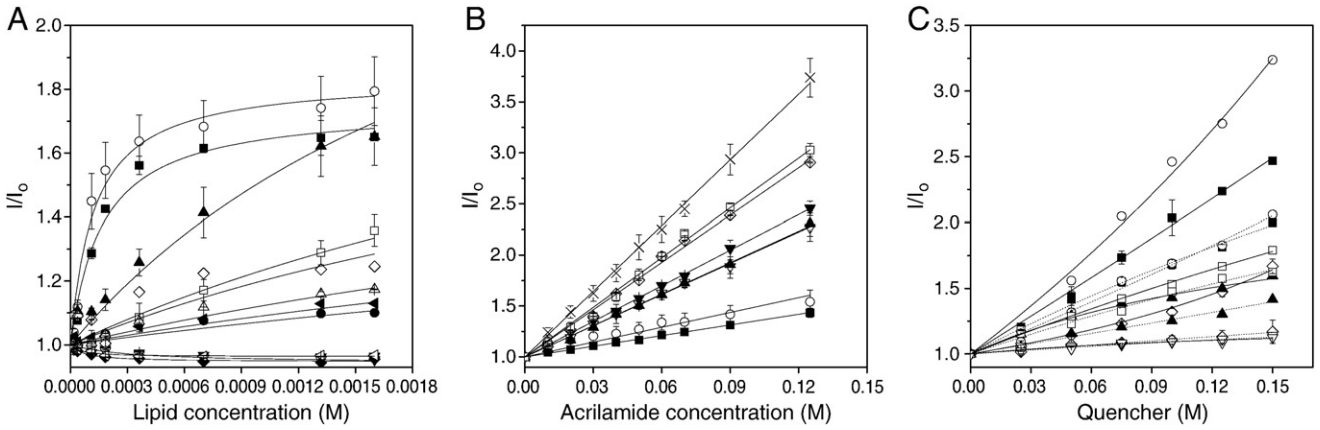

Fig. 2. (A) Change on the fluorescence intensity of the Trp residue of the $NS4B_{H1}$ peptide in the presence of increasing lipid concentration, (B) Stern–Volmer plots for the quenching of the fluorescence of the Trp residue of the $NS4B_{H1}$ peptide in the presence by acrylamide and (C) Stern–Volmer plots for the depth-dependent quenching of the fluorescence of the Trp residue of the $NS4B_{H1}$ peptide in the presence of the 5-NS and 16-NS probes. The lipid compositions used were ER (◀), EPC (▼), BPS/CHOL at a molar ratio of 5:1 (■), EPA/CHOL at a molar ratio of 5:1 (○), EPC/CHOL at a molar ratio of 5:1 (▽), EPC/ESM/CHOL at a molar ratio of 5:1:1 (♦), EPC/EPA at a molar ratio of 5:2 (▲), EPC/BPS at a molar ratio of 5:2 (□), EPC/BPS/CHOL at a molar ratio of 5:3:1 (●), EPC/TPE/CHOL at a molar ratio of 5:3:1 (◁), EPC/EPA/CHOL at a molar ratio of 5:3:1 (△), and EPC/ESM/CHOL at a molar ratio of 5:3:1 (◊). In (B), pure peptides are represented by (×). In (C) solid lines correspond to 5-NS and dotted lines to 16-NS. Vertical bars indicate standard deviations of the mean of triplicate samples. The lipid to peptide ratio was 100:1 for experiments using acrylamide and NS probes.

Table 2
Partition coefficients (K_P) and Stern–Volmer quenching constants (K_{SV}) obtained from the fluorescence of the Trp residue of the $NS4B_{H1}$ peptide in buffer and in the presence of different model membranes.

LUV COMPOSITION	K_P ($\times 10^{-5}$ M^{-1}) *Trp*	K_{sv} (M^{-1}) *Acrylamide*	K_{sv} (M^{-1}) *5-NS*	*16-NS*
BPS/CHOL 5:1	3.30 ± 0.6	3.50 ± 0.2	9.70 ± 0.9	9.3 ± 1.6
EPA/CHOL 5:1	4.50 ± 0.87	4.80 ± 0.2	10.2 ± 0.6	5.8 ± 1.1
EPC/CHOL 5:1	0.88 ± 0.5	10.2 ± 0.2	7.30 ± 0.2	2.8 ± 0.7
EPC	1.10 ± 0.9	11.6 ± 0.2	–	–
EPC/EPA 5:2	2.90 ± 0.1	10.3 ± 0.4	12.8 ± 3.4	2.4 ± 2.2
EPC/ESM/CHOL 5:3:1	1.14 ± 0.4	15.4 ± 0.7	1.93 ± 0.3	1.5 ± 0.5
EPC/BPS 5:2	1.09 ± 0.7	16.2 ± 0.8	7.40 ± 1.7	6.8 ± 1.9
EPC/ESM/CHOL 5:1:1	1.10 ± 0.91	–	–	–
EPC/TPE/CHOL 5:3:1	0.78 ± 0.51	–	–	–
EPC/EPA/CHOL 5:3:1	0.67 ± 0.11	–	–	–
EPC/BPS/CHOL 5:3:1	0.90 ± 0.26	–	–	–
ER complex mixture	0.47 ± 0.2	–	–	–
Buffer	–	21.4 ± 1.2	–	–

behavior. In aqueous solution the Trp residues were highly exposed to the solvent that led to a more efficient quenching. However, in the presence of the phospholipid membranes, the extent of quenching was significantly reduced, indicating a poor accessibility of the Trp residue to the aqueous phase, consistent with its incorporation into the lipid bilayer. The $NS4B_{H1SC}$ peptide in solution gave a K_{SV} of 11.3 M^{-1}, suggesting a lesser accessibility of the peptide Trp to the solvent than the $NS4B_{H1}$ peptide (K_{SV} of 21.4 M^{-1}), assuming invariance of the Trp lifetime. For the $NS4B_{H1}$ peptide, the extent of quenching was significantly reduced in the presence of negatively charged phospholipid membranes, in accordance with the results shown above. The transverse location (penetration) of the $NS4B_{H1}$ peptide in the lipid bilayer was evaluated by monitoring the relative quenching of the fluorescence of the Trp residue by the lipophylic spin probes 5NS and 16NS when the peptide was incorporated in the fluid phase of vesicles having different phospholipid compositions (Fig. 2C), whereas the K_{SV} values for both probes are presented in Table 2. In general, 16-NS quenches the peptides fluorescence less efficiently than 5-NS, but the difference between the two probes is not very high. These data allow us to conclude that the Trp residue resides in between these probes, but nearer to the 5-NS probe than to the 16-NS one.

3.4. Perturbation induced by the peptide in the lipid palisade

Membrane lipids undergo a cooperative melting reaction, which is linked to the loss of conformational order of the lipid chains and it has been known for a long time that the melting process of membrane lipids is influenced by many types of molecules including proteins and peptides. The effect of the $NS4B_{H1}$ peptide on the structural and thermotropic properties of phospholipid membranes was investigated by measuring the steady-state fluorescence anisotropy of the fluorescent probes DPH and TMA-DPH incorporated into model membranes composed of saturated synthetic phospholipids as a function of temperature (Fig. 3). DPH is known to partition mainly into the hydrophobic core of the membrane, whereas TMA-DPH is oriented at the membrane bilayer with its charge localized at the lipid-water interface [39]. Their different location and orientation in the membrane allows to analyze the effect of the $NS4B_{H1}$ peptide on the structural and thermotropic properties along the full length of the membrane. In the case of DMPC, the $NS4B_{H1}$ peptide decreased the cooperativity of the thermal transition and in addition elicited a shift of about 2–4 °C to lower temperatures of the T_m (Fig. 3A and B). However, the anisotropy of both DPH and TMA-DPH above and below the T_m of DMPC was not significantly changed. $NS4B_{H1}$ decreased the cooperativity of the phospholipid transition of DMPG, decreased and increased the anisotropy of both DPH and TMA-DPH below and above the T_m, but did not decrease significantly the temperature of the thermal transition of DMPG (Fig. 3C and D). The decrease in cooperativity of DMPG elicited by the peptide is perfectly visible in the derivative of the curves (inserts, Fig. 3C and D). For DMPS and DMPA bilayers, $NS4B_{H1}$ did not changed significantly the cooperativity of their respective transitions as well as the anisotropy below and above the T_m , but induced a shift of about 2–4 °C to lower temperatures of the T_m (Fig. 3E and F and Fig. 3G and H for DMPS and DMPA, respectively). $NS4B_{H1}$ was able of affecting the thermal transition T_m for all phospholipids as observed by both types of probes, was able to perturb the phospholipid acyl chains and therefore should be located at the lipid-water interface influencing the fluidity of the phospholipids [28]. The difference in charge between the phospholipid head-groups affects but slightly the peptide incorporation into the lipid bilayer.

As noted above, it seems that there is a specific interaction between the $NS4B_{H1}$ peptide and sphingomyelin. Because of that we have also studied the effect of the $NS4B_{H1}$ peptide on the thermotropic phase behavior of phospholipid multilamellar vesicles containing either ESM or PSM using differential scanning calorimetry (DSC). The corresponding profiles are shown in Fig. 4. DMPC, which have not been extensively annealed at low temperatures, displays two endothermic peaks on heating, the pre-transition (12–14 °C, $L_{\beta'}$–$P_{\beta'}$) and the main transition (24 °C, $P_{\beta'}$–L_α). As illustrated in Fig. 4A, incorporation of $NS4B_{H1}$ at a lipid/peptide ratio of 15:1 significantly altered the thermotropic behavior of DMPC, since the peptide abolished completely the pre-transition of the phospholipid, as well as significantly broadened the transition of DMPC in accordance with the anisotropy results commented above. The main transition is apparently composed of at least two different peaks, which should be due to mixed phases. In a similar way, incorporation of $NS4B_{H1}$ into PSM membranes at a lipid/peptide ratio of 15:1 significantly altered the thermotropic behavior of the phospholipid (Fig. 4B). The peptide broadened the main transition of PSM and apparently gave place to at least two different peaks, which should be also due to mixed phases. Incorporation of $NS4B_{H1}$ into binary membranes composed of DMPC/ESM and DMPC/PSM at molar ratios of 5:3 changed considerably the thermotropic behavior of the mixtures (Fig 4C and D). The slightly broad transition of the binary mixture was broadened by the presence of the peptide and, at lipid/peptide molar ratios of 5:1, three thermotropic transitions were noticeable: at about 28, 35 and 46 °C. The first transition should correspond to a phase enriched in DMPC, the second one to a phase consisting of a mixture of both DMPC and either ESM or PSM and the third one to a phase enriched in either ESM or PSM. The coexistence of different phases induced by the presence of $NS4B_{H1}$ would indicate that one of them would be enriched in peptide (phospholipids highly disturbed) whereas the other ones would be impoverished in them (phospholipids slightly disturbed).

3.5. Secondary structure of the $NS4B_{H1}$ peptide

The existence of structural changes on the $NS4B_{H1}$ peptide induced by membrane binding was studied by analyzing the infrared Amide I′ band located between 1700 and 1600 cm^{-1}. The Amide I′ region of the fully hydrated peptide in buffer is shown in Fig. 5A. For the peptide in solution and at low temperatures, the Amide I′ band was asymmetric with a maximum at about 1647 cm^{-1} and one shoulder at about 1672 cm^{-1}. The broad band with the intensity maxima at about 1647 cm^{-1} would mainly correspond to a mixture of unordered and helical structures, whereas the band with the intensity maxima at about 1672 cm^{-1} would correspond to β-sheet [40,41]. Increasing the temperature, the band with the maximum at 1647 cm^{-1} slightly broadened and increased in frequency to about 1649 cm^{-1} (Fig. 5E) and at the same time a shoulder appeared at about 1615 cm^{-1}, which would correspond to aggregated structures (Fig. 5A). These data would imply that the $NS4B_{H1}$ peptide changed from a mixture of helical, unordered and β-sheet structures at low temperatures to a mixture of helical,

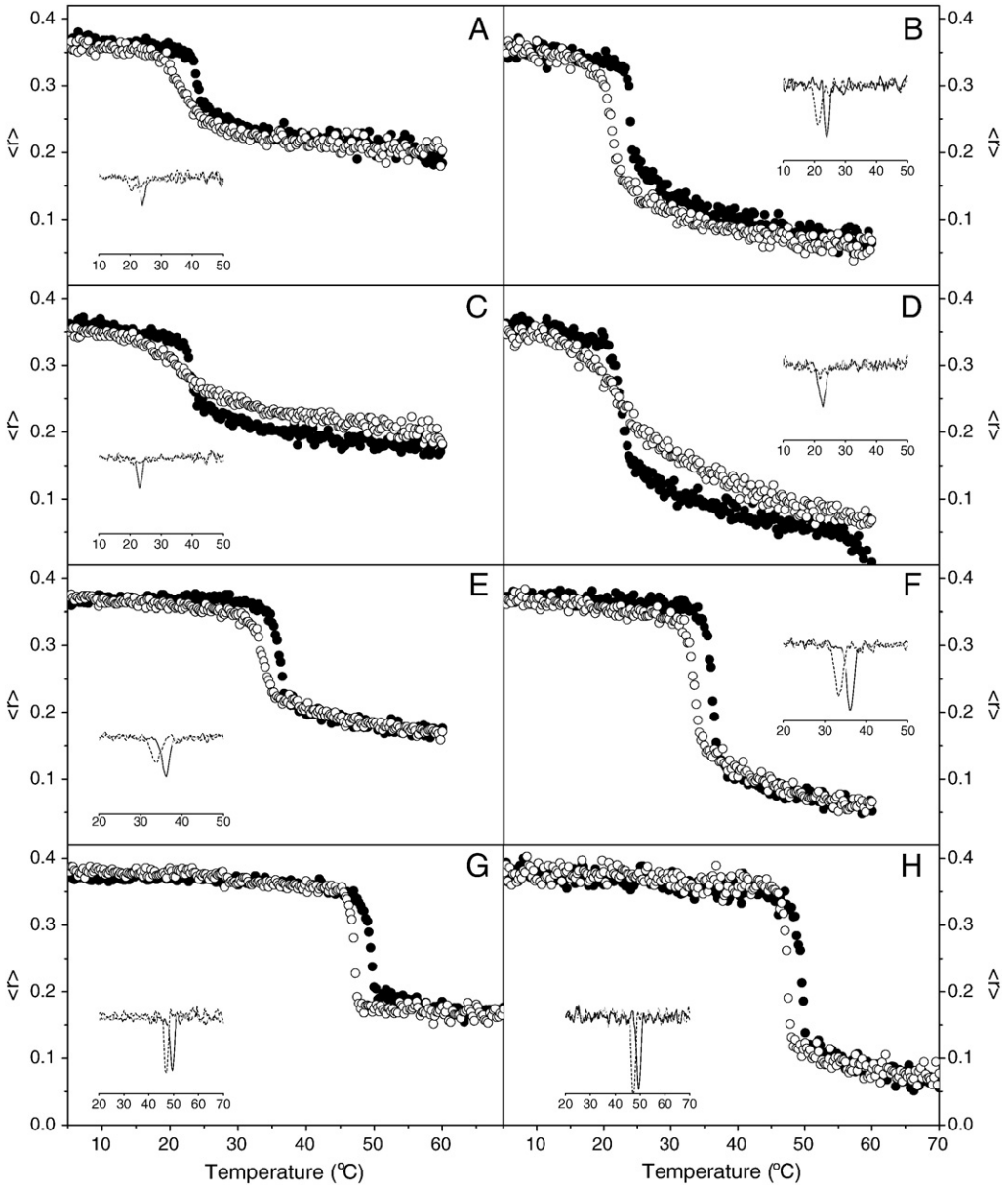

Fig. 3. Steady-state anisotropy, <r>, of TMA-DPH (A, C, E and G) and DPH (B, D, F and H) incorporated into (A and B) DMPC, (C and D) DMPG , (E and F) DMPS and (G and H) DMPA model membranes as a function of temperature. Data correspond to vesicles containing pure phospholipid (●) and phospholipid plus $NS4B_{H1}$ peptide at a 15:1 molar ratio (○). The inserts show the normalized 13-point smoothed first derivative of the curves.

unordered, β-sheet and aggregated structures at high temperatures. Furthermore, this transitional change in overall structure occurs at about 42–48 °C (Fig. 5E).

In the presence of DMPC and at low temperatures, the Amide I′ envelope of $NS4B_{H1}$ was similar to that observed for the peptide in solution (Fig. 5B). However, at approximately 42 °C a band at approximately 1615 cm^{-1} was apparent; this band increased in intensity as the temperature increased and at the same time the broad band at 1646 cm^{-1} decreased in intensity with no change above 60 °C (Fig. 5B and F). These changes in band intensity show that $NS4B_{H1,}$ in the presence of DMPC, presents a high percentage of unordered and helical structures at low temperatures but a high percentage of aggregated structures at higher ones. The maximum of the ester C = O band of DMPC in the presence of $NS4B_{H1}$, displayed two broad transitions, one between 20 and 28 °C (from 1738 cm^{-1} to 1734 cm^{-1}) and another one at about 42–60 °C (from 1734 cm^{-1} to 1732 cm^{-1}). The first broad transition which appears at about 20–28 °C coincides with the gel-to-liquid crystalline phase transition of DMPC (see Fig. 3C and D), whereas the second broad 42–60 °C transition coincides with the structural change of $NS4B_{H1}$ commented above. These results imply that $NS4B_{H1}$ affects the molecule of DMPG and at the same DMPG affects the $NS4B_{H1}$ peptide.

In the presence of DMPG and at low temperatures, the Amide I′ envelope of $NS4B_{H1}$ was similar to that observed for the peptide in solution at relatively high temperatures, with a broad band at about 1646 cm^{-1} and a shoulder at about 1615 cm^{-1} (Fig. 5C). The relative intensity of the two bands changed as the temperature increased giving place to three broad transitions, i.e., about 22 °C, 44 °C and 60 °C (Fig. 5C and G). These changes in band intensity show that $NS4B_{H1,}$ in the presence of DMPG, oscillates between a mixture of unordered and helical structures and a mixture of unordered, helical and aggregated structures. The ester C = O band of DMPG in the presence of $NS4B_{H1}$ presented two maxima at about 1738 cm^{-1} and 1723 cm^{-1} at low temperatures (Fig. 5C). These two relatively sharp bands coalesced into a broad band which changed in frequency as the temperature increased; this broad C = O band of DMPG showed two

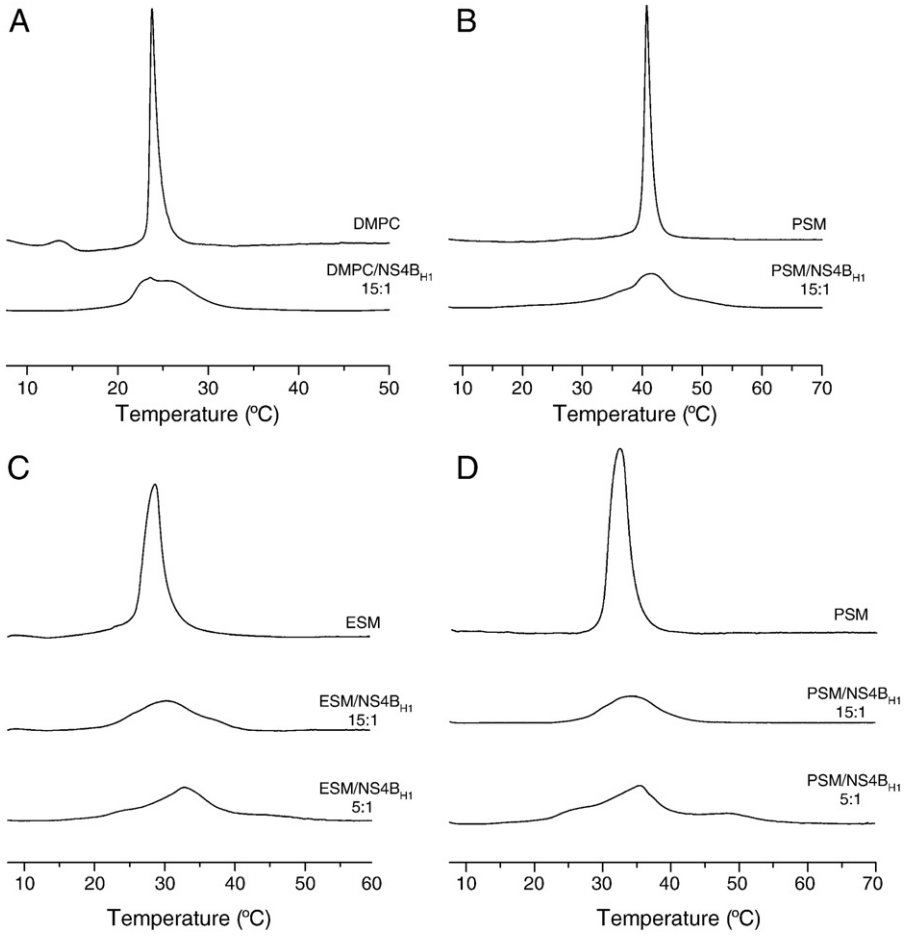

Fig. 4. Differential scanning calorimetry heating-scan thermograms for (A) DMPC and DMPC/NS4B$_{H1}$ 15:1, (B) PSM and PSM/NS4B$_{H1}$ at a molar ratio of 15:1, (C) ESM, ESM/NS4B$_{H1}$ at a molar ratio of 15:1, and ESM/NS4B$_{H1}$ at a molar ratio of 5:1, and (D) PSM, PSM/NS4B$_{H1}$ at a molar ratio of 15:1, and PSM/NS4B$_{H1}$ at a molar ratio of 5:1. All thermograms were normalized to the same amount of lipid.

transitions, one at about 45 °C and another one at about 60 °C. (Fig. 5G). DMPG, as a phosphatidylglycerol phospholipid, can exhibit under physiologically relevant conditions a more complex pattern of thermotropic phase behavior than the corresponding zwitterionic phosphatidylcholine DMPC, which could include the formation of one or more high melting crystalline or quasi-crystalline lamellar phases and the formation of extended three-dimensional bilayer networks where curvature elasticity is of primary relevance [42,43].The pattern of thermotropic phase behavior exhibited by freshly dispersed samples of DMPG is remarkably similar to that of DMPC. However, incubation of phosphatidylglycerols at low temperatures results in the formation of one or more quasi-crystalline structures at rates dependent on the hydrocarbon chain length, i.e., L_c1b and L_c2 phases [42,43]. The appearance of two sharps C=O bands in DMPG at relatively low temperatures, as shown in Fig. 5C, suggest that a new phase, likely the L_c1b phase, is induced at low temperatures by the presence of the NS4B$_{H1}$ peptide. These results show that both types of molecules, NS4B$_{H1}$ and DMPG, sense at the same time all these transitions, i.e., both types of molecules affect each other, a new phase is induced at low temperatures, and furthermore, these interactions might have large implications for different biological processes and particularly to membrane perturbation.

The Amide I′ envelope of NS4B$_{H1}$ in the presence of DMPA displayed a intense narrow band at about 1616 cm^{-1}, a broad band with a maximum at about 1645 cm^{-1}, and two small bands at about 1684 and 1670 cm^{-1} (Fig. 5D). The bands at about 1685 and 1616 cm^{-1} should correspond to aggregated structures, the broad band at about 1645 cm^{-1} would mainly correspond to a mixture of unordered and helical structures, whereas the band at about 1670 cm^{-1} would correspond to β-sheet structures [40,41]. Increasing the temperature, a change in frequency is apparent in the narrow band, since it moves from about 1615 to 1623 cm^{-1} with a transition between 70 and 74 °C, at the same time that the small band at 1685 cm^{-1} disappears and the other small band at 1670 cm^{-1} moves to about 1674 cm^{-1} (Fig. 5D and H). The disappearance of the band at 1685 cm^{-1} with a concomitant change from the band at 1615 to 1623 cm^{-1} indicates that the aggregated structures transform most probably to β-sheet structures [40,41]. The maximum of the ester C=O band of DMPA in the presence of NS4B$_{H1}$ displayed two transitions, one beginning at about 51 °C (from 1738 to 1735 cm^{-1}) and the other one beginning at about 68 °C (from 1735 to 1732 cm^{-1}) (Fig. 5H). The first transition is related to the gel-to-liquid crystalline phase transition of DMPA (see Fig. 3), whereas the second broad one coincides with the structural change of NS4B$_{H1}$ commented above. These results imply that NS4B$_{H1}$ affects the DMPA molecule and at the same DMPA affects the secondary structure of the NS4B$_{H1}$ peptide.

4. Discussion

The replication and assembly of HCV, which remains essentially unclear, has been suggested to occur in the ER or ER-derived membranes [8–10,44]. Most, if not all, of the HCV NS proteins including NS4B, play a central role in viral particle formation and budding, but their specific function in replication and/or assembly remains poorly understood [6,7]. NS4B, a highly hydrophobic protein, has been suggested to alter ER membranes so that the HCV replication complex can be formed and therefore has a critical role in HCV formation. Since the biological role/

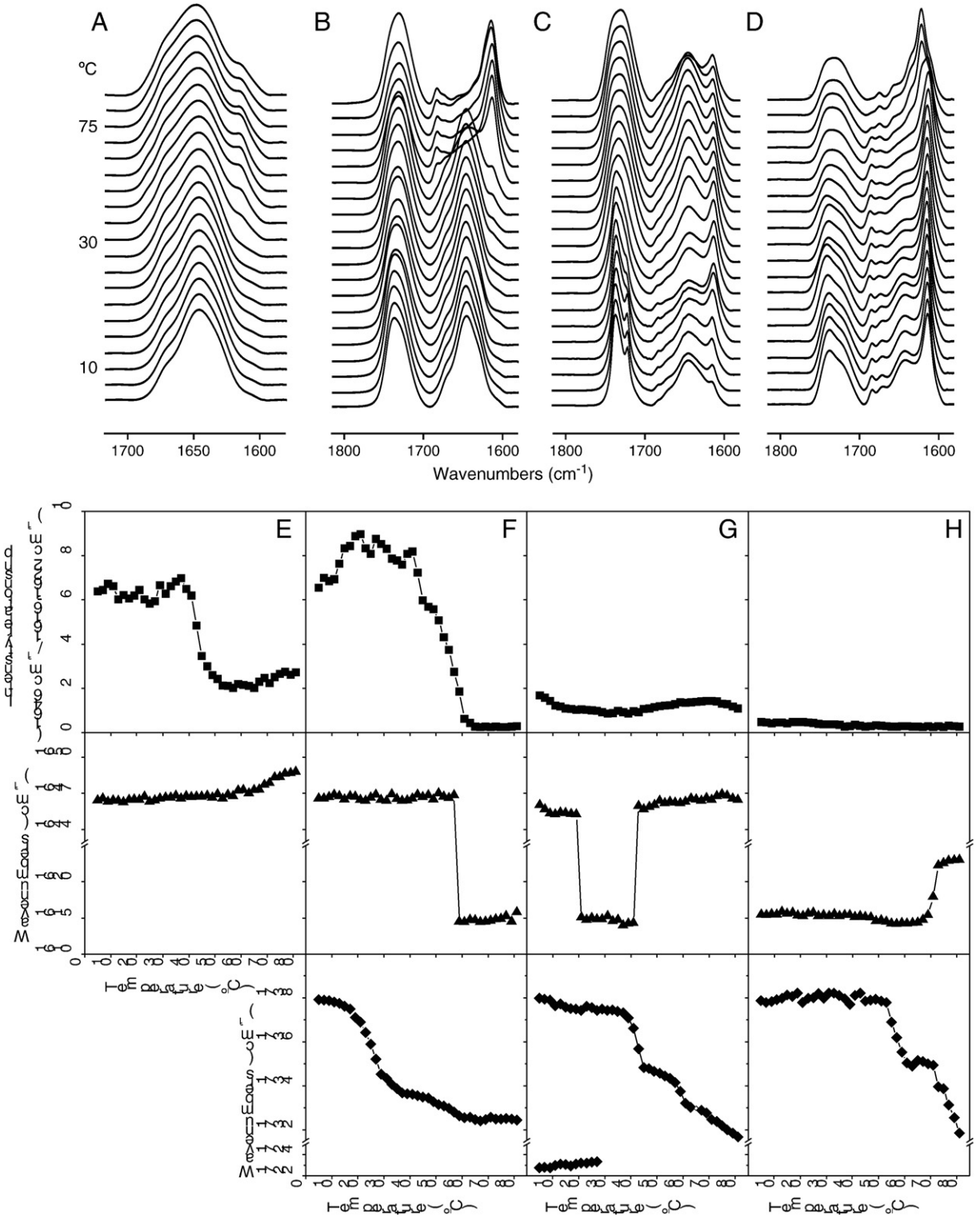

Fig. 5. Stacked infrared spectra in the C = O and Amide I′ region for the $NS4B_{H1}$ peptide in solution (A) and in the presence of DMPC (B), DMPG (C) and DMPA (D) at different temperatures as indicated. The phospholipid-to-peptide molar ratio was 15:1. The temperature dependence of the 1646 cm^{-1}/1616 cm^{-1} intensity relationship (■), Amide I′ maximum (▲) and C = O maximum (♦) for the $NS4B_{H1}$ peptide in solution and in the presence of DMPC, DMPG and DMPA are shown in E, F, G and H, respectively. See text for details.

roles of NS4B is/are intrinsically united to the membrane, we have extended our previous work [19] to investigate the binding and interaction of the membranotropic highly conserved H1 region of NS4B, i.e., peptide $NS4B_{H1}$, with membrane model systems. We have carried out an in-depth biophysical study aimed to elucidate the capacity of this region to interact and disrupt membranes, as well as to study the structural and dynamic features which might be relevant for that disruption. Our findings give some clues to a key region in the viral protein that might be implicated in the HCV life cycle, and therefore could be used as a new target for searching inhibitors of viral replication and assembly.

The $NS4B_{H1}$ peptide was capable of altering membrane stability causing the release of fluorescent probes, this effect being dependent on lipid composition and on the lipid/peptide molar ratio. The highest

release was observed for liposomes containing negatively charged phospholipids, although significant leakage values were also observed for liposomes composed of zwitterionic phospholipids. A scrambled peptide did not induce membrane leakage at all, indicating that the specific sequence of $NS4B_{H1}$ is fundamental to observe any effect. Interestingly, the ESM and CHOL content also modulated membrane rupture, since ESM increased but CHOL decreased the leakage extent. This differences could be a consequence of influence of cholesterol in the membrane penetration of peptides attenuating its insertion as it has been observed for other peptides [45]. These results were corroborated by using a specific ER complex membrane, indicating that the specific disrupting effect elicited by the $NS4B_{H1}$ peptide should depend on the phospholipid head-group characteristics, i.e., charge and possibly hydrogen bonding, although hydrophobic interactions within the bilayer should not be ruled out. The fact that the scrambled peptide did not interact in the same way with the membrane supports the importance of the specificity on the primary amino acid sequence of this peptide.

We have also shown that the $NS4B_{H1}$ peptide binds with high affinity to phospholipid model membranes, as it has been similarly found for other peptides [36,38]. Binding was further demonstrated by hydrophilic quenching probes, since the $NS4B_{H1}$ peptide was less accessible for quenching by acrylamide implying a buried location. The lipophylic probe quenching results suggest a shallow-to-intermediate location of the peptide in the membrane, but the extent of quenching is relatively low compared to other peptides [30,46,47]. Interestingly, these data suggest that the insertion of the peptide into the bilayer palisade depends on phospholipid composition. We have also shown that the $NS4B_{H1}$ peptide is capable of affecting the steady-state fluorescence anisotropy of fluorescent probes located into the palisade structure of the membrane, since the peptide was able of decreasing the mobility and cooperativity of the phospholipid acyl chains when compared to the pure phospholipids. Calorimetry experiments further corroborated these results, and additionally indicated that the $NS4B_{H1}$ peptide induced the presence of mixed lipid phases, enriched and impoverished in peptide. This result strengthens that the location of the peptide is at or near the membrane interface, influencing the fluidity of the phospholipids, most probably with an in-plane orientation rather than in a transmembrane position [48].

The infrared spectra of the Amide I′ region of the fully hydrated peptide in solution at low temperatures displayed a coexistence of α-helix, β-sheet and random structures; at about 42–48 °C a broad transition with a concomitant increase in aggregated structures occurred. In the presence of different types of phospholipids as well as at different temperatures, different amounts of secondary structures were found. At the same time, differences in the frequency and number of bands corresponding to the carbonyl band of the phospholipids were observed. However, and most important, the changes which were observed were coincidental with each other, implying that both types of molecules affected one to the other and vice versa. These results imply that the secondary structure of the $NS4B_{H1}$ peptide was affected by its binding to the membrane, so that membrane binding modulates the secondary structure of the peptide as it has been suggested for other peptides [19,49].

The binding of peptide $NS4B_{H1}$ to the surface of the membrane and the modulation of the phospholipid biophysical properties which takes place as a consequence of binding could be related to the conformational changes which might occur during the biological activity of the NS4B protein. Consequently the NS4B region where peptide $NS4B_{H1}$ resides might have an essential role in the membrane replication and/or assembly of the viral particle through the modulation of the membrane structure and hence the replication complex. The conservation of its structure as well as its physical and chemical properties should be essential in its function, since changes in the primary sequence prevent the resulting peptide from interacting with the membrane. Our results add new information about how this region can contribute to the interaction with the membrane. Although the peptide is not deeply buried in the membrane, its interaction with the membrane depends on its composition and it is able to affect the lipid milieu from the membrane surface down to the hydrophobic core. Consequently, our results identify an important region in the HCV NS4B protein which might be directly implicated in the HCV life cycle. Additionally, pharmacological disruption of NS4B interaction with membranes could represent the basis for a novel approach to anti-HCV therapy.

Acknowledgements

This work was supported by grant BFU2008-02617-BMC (Ministerio de Ciencia y Tecnología, Spain) to J.V.

References

[1] D.M. Morens, G.K. Folkers, A.S. Fauci, The challenge of emerging and re-emerging infectious diseases, Nature 430 (2004) 242–249.
[2] Hepatitis C–global prevalence (update), Wkly Epidemiol Rec 75 (2000) 18–19.
[3] H. Tang, H. Grise, Cellular and molecular biology of HCV infection and hepatitis, Clin. Sci. (Lond) 117 (2009) 49–65.
[4] S.A. Qureshi, Hepatitis C virus-biology, host evasion strategies, and promising new therapies on the horizon, Med. Res. Rev. 27 (2007) 353–373.
[5] C. Vauloup-Fellous, V. Pene, J. Garaud-Aunis, F. Harper, S. Bardin, Y. Suire, E. Pichard, A. Schmitt, P. Sogni, G. Pierron, P. Briand, A.R. Rosenberg, Signal peptide peptidase-catalyzed cleavage of hepatitis C virus core protein is dispensable for virus budding but destabilizes the viral capsid, J. Biol. Chem. 281 (2006) 27679–27692.
[6] D. Moradpour, F. Penin, C.M. Rice, Replication of hepatitis C virus, Nat. Rev. Microbiol. 5 (2007) 453–463.
[7] M. Dimitrova, I. Imbert, M.P. Kieny, C. Schuster, Protein-protein interactions between hepatitis C virus nonstructural proteins, J. Virol. 77 (2003) 5401–5414.
[8] N. El-Hage, G. Luo, Replication of hepatitis C virus RNA occurs in a membrane-bound replication complex containing nonstructural viral proteins and RNA, J. Gen. Virol. 84 (2003) 2761–2769.
[9] R. Gosert, D. Egger, V. Lohmann, R. Bartenschlager, H.E. Blum, K. Bienz, D. Moradpour, Identification of the hepatitis C virus RNA replication complex in Huh-7 cells harboring subgenomic replicons, J. Virol. 77 (2003) 5487–5492.
[10] G. Mottola, G. Cardinali, A. Ceccacci, C. Trozzi, L. Bartholomew, M.R. Torrisi, E. Pedrazzini, S. Bonatti, G. Migliaccio, Hepatitis C virus nonstructural proteins are localized in a modified endoplasmic reticulum of cells expressing viral subgenomic replicons, Virology 293 (2002) 31–43.
[11] T. Hugle, F. Fehrmann, E. Bieck, M. Kohara, H.G. Krausslich, C.M. Rice, H.E. Blum, D. Moradpour, The hepatitis C virus nonstructural protein 4B is an integral endoplasmic reticulum membrane protein, Virology 284 (2001) 70–81.
[12] G.Y. Yu, K.J. Lee, L. Gao, M.M. Lai, Palmitoylation and polymerization of hepatitis C virus NS4B protein, J. Virol. 80 (2006) 6013–6023.
[13] D.M. Jones, A.H. Patel, P. Targett-Adams, J. McLauchlan, The hepatitis C virus Ns4b protein can trans-complement viral RNA replication and modulates production of infectious virus, J. Virol. (2008).
[14] D. Egger, B. Wolk, R. Gosert, L. Bianchi, H.E. Blum, D. Moradpour, K. Bienz, Expression of hepatitis C virus proteins induces distinct membrane alterations including a candidate viral replication complex, J. Virol. 76 (2002) 5974–5984.
[15] M. Lundin, M. Monne, A. Widell, G. Von Heijne, M.A. Persson, Topology of the membrane-associated hepatitis C virus protein NS4B, J. Virol. 77 (2003) 5428–5438.
[16] M. Elazar, P. Liu, C.M. Rice, J.S. Glenn, An N-terminal amphipathic helix in hepatitis C virus (HCV) NS4B mediates membrane association, correct localization of replication complex proteins, and HCV RNA replication, J. Virol. 78 (2004) 11393–11400.
[17] C. Welsch, M. Albrecht, J. Maydt, E. Herrmann, M.W. Welker, C. Sarrazin, A. Scheidig, T. Lengauer, S. Zeuzem, Structural and functional comparison of the non-structural protein 4B in flaviviridae, J. Mol. Graph. Model. 26 (2007) 546–557.
[18] S.M. Lemon, J.A. McKeating, T. Pietschmann, D.N. Frick, J.S. Glenn, T.L. Tellinghuisen, J. Symons, P.A. Furman, Development of novel therapies for hepatitis C, Antiviral Res 86 79–92.
[19] J. Guillen, A. Gonzalez-Alvarez, J. Villalain, A membranotropic region in the C-terminal domain of Hepatitis C virus protein NS4B Interaction with membranes, Biochim. Biophys. Acta 1798 (2010) 327–337.
[20] W.K. Surewicz, H.H. Mantsch, D. Chapman, Determination of protein secondary structure by Fourier transform infrared spectroscopy: a critical assessment, Biochemistry 32 (1993) 389–394.
[21] Y.P. Zhang, R.N. Lewis, R.S. Hodges, R.N. McElhaney, FTIR spectroscopic studies of the conformation and amide hydrogen exchange of a peptide model of the hydrophobic transmembrane alpha-helices of membrane proteins, Biochemistry 31 (1992) 11572–11578.
[22] A.G. Krainev, D.A. Ferrington, T.D. Williams, T.C. Squier, D.J. Bigelow, Adaptive changes in lipid composition of skeletal sarcoplasmic reticulum membranes associated with aging, Biochim. Biophys. Acta 1235 (1995) 406–418.

[23] L.D. Mayer, M.J. Hope, P.R. Cullis, Vesicles of variable sizes produced by a rapid extrusion procedure, Biochim. Biophys. Acta 858 (1986) 161–168.
[24] C.S.F. Böttcher, C.M. Van Gent, C. Fries, A rapid and sensitive sub-micro phosphorus determination, Anal. Chim. Acta 1061 (1961) 203–204.
[25] H. Edelhoch, Spectroscopic determination of tryptophan and tyrosine in proteins, Biochemistry 6 (1967) 1948–1954.
[26] A. Bernabeu, J. Guillen, A.J. Perez-Berna, M.R. Moreno, J. Villalain, Structure of the C-terminal domain of the pro-apoptotic protein Hrk and its interaction with model membranes, Biochim. Biophys. Acta 1768 (2007) 1659–1670.
[27] M.R. Moreno, J. Guillen, A.J. Perez-Berna, D. Amoros, A.I. Gomez, A. Bernabeu, J. Villalain, Characterization of the interaction of two peptides from the N terminus of the NHR domain of HIV-1 gp41 with phospholipid membranes, Biochemistry 46 (2007) 10572–10584.
[28] L.M. Contreras, F.J. Aranda, F. Gavilanes, J.M. Gonzalez-Ros, J. Villalain, Structure and interaction with membrane model systems of a peptide derived from the major epitope region of HIV protein gp41: implications on viral fusion mechanism, Biochemistry 40 (2001) 3196–3207.
[29] J. Guillen, R.F. Almeida, M. Prieto, J. Villalain, Structural and dynamic characterization of the interaction of the putative fusion peptide of the S2 SARS-CoV virus protein with lipid membranes, J. Phys. Chem. B (2008).
[30] J. Guillen, M.R. Moreno, A.J. Perez-Berna, A. Bernabeu, J. Villalain, Interaction of a peptide from the pre-transmembrane domain of the severe acute respiratory syndrome coronavirus spike protein with phospholipid membranes, J. Phys. Chem. B 111 (2007) 13714–13725.
[31] J. Lakowicz, Principles of fluorescence spectroscopy, Kluwer-Plenum Press, New York, 1999.
[32] T.C. Laurent, K.A. Granath, Fractionation of dextran and Ficoll by chromatography on Sephadex G-200, Biochim. Biophys. Acta 136 (1967) 191–198.
[33] D.B. Fisher, C.E. Cash-Clark, Sieve tube unloading and post-phloem transport of fluorescent tracers and proteins injected into sieve tubes via severed aphid stylets, Plant Physiol. 123 (2000) 125–138.
[34] H. Aizaki, K.J. Lee, V.M. Sung, H. Ishiko, M.M. Lai, Characterization of the hepatitis C virus RNA replication complex associated with lipid rafts, Virology 324 (2004) 450–461.
[35] S.T. Shi, K.J. Lee, H. Aizaki, S.B. Hwang, M.M. Lai, Hepatitis C virus RNA replication occurs on a detergent-resistant membrane that cofractionates with caveolin-2, J. Virol. 77 (2003) 4160–4168.
[36] R. Pascual, M. Contreras, A. Fedorov, M. Prieto, J. Villalain, Interaction of a peptide derived from the N-heptad repeat region of gp41 Env ectodomain with model membranes. Modulation of phospholipid phase behavior, Biochemistry 44 (2005) 14275–14288.
[37] N.C. Santos, M. Prieto, M.A. Castanho, Interaction of the major epitope region of HIV protein gp41 with membrane model systems. A fluorescence spectroscopy study, Biochemistry 37 (1998) 8674–8682.
[38] R. Pascual, M.R. Moreno, J. Villalain, A peptide pertaining to the loop segment of human immunodeficiency virus gp41 binds and interacts with model biomembranes: implications for the fusion mechanism, J. Virol. 79 (2005) 5142–5152.
[39] B.R. Lentz, Use of fluorescent probes to monitor molecular order and motions within liposome bilayers, Chem. Phys. Lipids 64 (1993) 99–116.
[40] J.L. Arrondo, F.M. Goni, Structure and dynamics of membrane proteins as studied by infrared spectroscopy, Prog. Biophys. Mol. Biol. 72 (1999) 367–405.
[41] D.M. Byler, H. Susi, Examination of the secondary structure of proteins by deconvolved FTIR spectra, Biopolymers 25 (1986) 469–487.
[42] P. Garidel, A. Blume, W. Hubner, A Fourier transform infrared spectroscopic study of the interaction of alkaline earth cations with the negatively charged phospholipid 1, 2-dimyristoyl-sn-glycero-3-phosphoglycerol, Biochim. Biophys. Acta 1466 (2000) 245–259.
[43] R.M. Epand, B. Gabel, R.F. Epand, A. Sen, S.W. Hui, A. Muga, W.K. Surewicz, Formation of a new stable phase of phosphatidylglycerols, Biophys. J. 63 (1992) 327–332.
[44] M. Ait-Goughoulte, C. Hourioux, R. Patient, S. Trassard, D. Brand, P. Roingeard, Core protein cleavage by signal peptide peptidase is required for hepatitis C virus-like particle assembly, J. Gen. Virol. 87 (2006) 855–860.
[45] H. Zhao, R. Sood, A. Jutila, S. Bose, G. Fimland, J. Nissen-Meyer, P.K. Kinnunen, Interaction of the antimicrobial peptide pheromone Plantaricin A with model membranes: implications for a novel mechanism of action, Biochim. Biophys. Acta 1758 (2006) 1461–1474.
[46] M.R. Moreno, A.J. Perez-Berna, J. Guillen, J. Villalain, Biophysical characterization and membrane interaction of the most membranotropic region of the HIV-1 gp41 endodomain, Biochim. Biophys. Acta (2008).
[47] A.J. Perez-Berna, J. Guillen, M.R. Moreno, A.I. Gomez-Sanchez, G. Pabst, P. Laggner, J. Villalain, Interaction of the most membranotropic region of the HCV E2 envelope glycoprotein with membranes, Biophys. characterization Biophys. J. (2008).
[48] F. Penin, V. Brass, N. Appel, S. Ramboarina, R. Montserret, D. Ficheux, H.E. Blum, R. Bartenschlager, D. Moradpour, Structure and function of the membrane anchor domain of hepatitis C virus nonstructural protein 5A, J. Biol. Chem. 279 (2004) 40835–40843.
[49] M.F. Palomares-Jerez, J. Guillen, J. Villalain, Interaction of the N-terminal segment of HCV protein NS5A with model membranes, Biochim. Biophys. Acta 1798 (2010) 1212–1224.